International Journal of Engineering Science 48 (2010) 15–20

Contents lists available at ScienceDirect

International Journal of Engineering Science

journal homepage: www.elsevier.com/locate/ijengsci

Charged wall growth in channel flow

T.I. Zohdi *

Department of Mechanical Engineering, University of California, Berkeley, CA, 94720-1740, USA

ARTICLE INFO

Article history:
Received 11 February 2009
Received in revised form 4 June 2009
Accepted 17 June 2009
Available online 18 July 2009

Communicated by M. Kachanov

Keywords:
Flow reduction
Wall growth
Charged fluids

ABSTRACT

The primary objective of this communication is to qualitatively describe charged wall growth in channel flow. The reduction of channel flow cross-section is often attributed to microscale suspensions and dissolved minerals which adhere to the flow boundaries (walls). In this analysis, the wall is comprised of an electrically conductive material, capable of carrying a charge. The flowing fluid, containing ions, is also assumed to be capable of carrying a charge. The resulting electrical field can be determined using Gauss' law, which allows the associated electrical force to be computed at the solid–fluid interface. This force can impede or enhance the attachment of suspensions to the wall. Thus, there are two effects that play a role at the charged solid–fluid interface/wall: (1) mechanical shear due to the fluid flow and (2) an electrical force. It is the goal of this communication to develop a relationship that characterizes both contributions and to ascertain how this relationship scales with wall growth.

1. Introduction/motivation

In this work, the dominant flow characteristics associated with growth of scale on electrically charged walls are modeled for a simple channel flow problem. The approach is to develop rate equations for the reduction of flow cross-sectional area as a function of the wall shear stress and charge distribution. Classical models for fully developed laminar and turbulent flows are employed. The strength of the applied electrical field is explicitly determined as a function of the flow radius and system parameters. The model captures two main effects, namely, for increasing scale build-up (smaller flow radius), the wall growth is limited by an accompanying rise in the fluid-induced wall shear stress, due to the more turbulent flow, while for smaller scale build-up (larger flow radius), electric field effects dominate the wall growth.

For the purposes of this work, the exact electrochemistry mechanism is unimportant, since the effects will be described phenomenologically.[1] Regardless of the exact mechanism of effective growth, it is influenced by the intensity of the shear stress near the wall. High shear stresses tend to impede material from adhering to the wall, while low shear stresses allow for relatively more wall growth. Also, the strength of the electrical field at the solid–fluid interface/wall contributes to the rate of growth. Consequently, there can be two competing effects (mechanical and electrical) controlling wall growth.

Electrical, galvanic-type, control of scale build-up has been widely used in industry for many years. *However, another possible application of electrically-based control of growth is through lightly charging biological tissue, for example, to mitigate plaque build-up in artery walls.* In this case, the objective would be to determine the lowest level of charging which would impede

* Tel.: +1 512 642 9172.
E-mail address: zohdi@newton.berkeley.edu

[1] For example, if the channel wall was negatively charged, there will be an electric force between the charged channel wall and counterions and polarized water molecules in the water near the channel wall. The basic idea is that this electric force serves to deter (or increase) the build-up of scale within the channel. Both electrical and magnetic approaches have been pursued in the realm of corrosion and scale mitigation via electrochemical manipulation at the wall boundary. For example, see the extensive works of Waskaas and co-workers [13,18–21].

0020-7225/$ - see front matter © 2009 Elsevier Ltd. All rights reserved.
doi:10.1016/j.ijengsci.2009.06.004

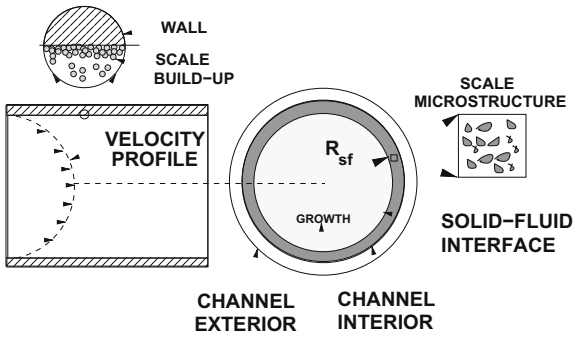

Fig. 1. Flow through a channel with wall growth.

detrimental growth and minimize electrically-induced tissue damage.[2] Clearly, *if implemented properly, in a minimally-invasive manner*, the electrochemistry at the artery wall can be controlled to mitigate plaque build-up, perhaps, for example, with the application of a (topical) patch on the surface of critical regions in the neck, similar to widely used patch-based drug-delivery systems.

2. Elementary qualitative models

Consider an idealized channel with a circular cross-section of (initial) area A_0 with an interior radius R_0 (Fig. 1). The objective is to describe the mechanism by which A_0 changes, via a reduction in R_0, due to wall growth caused by microscale deposits building up onto the channel's interior surface. The interior channel (solid–fluid interface) radius, denoted R_{sf}, changes over time $(R_{sf}(t=0)=R_0)$. Fully developed (incompressible) flow profiles, with constant overall flow rate $(Q_0 = v_0 A_0 = \int_A v\,dA = Q)$, are assumed, with a velocity given by

$$v = v_{\max}\left(1-\left(\frac{r}{R_{sf}}\right)^q\right). \tag{2.1}$$

For fully developed laminar flow, $q=2$, while for increasing q one characterizes, phenomenologically, progressively turbulent flow $(q \geqslant 2)$. The shear stress is given by $\tau = \mu\frac{\partial v}{\partial r}$. The value of the maximum profile velocity can be determined to be[3]

$$v_{\max} = \frac{Q_0(q+2)}{Aq}. \tag{2.2}$$

Therefore, shear stress at the wall, $r = R_{sf}$, is given by

$$|\tau_{nw}| = \left|\mu\frac{\partial v}{\partial r}\Big|_{R_{sf}}\right| = \left|\mu\frac{Q_o(q+2)}{\pi R_{sf}^3}\right|. \tag{2.3}$$

The tendency for material to adhere to the wall is controlled by the intensity of the shear stress near the wall. Higher shear stresses reduce the likelihood of material adhering to the wall, while lower shear stresses increase the tendency of material to adhere to the wall. Accordingly, we consider a growth law where the rate of growth is proportional to the difference between the shear stress near the wall and the critical "detachment" stress (τ^*), namely

$$\dot{R}_{sf} = \eta(|\tau_{nw}| - \tau^*) = \eta\left(\frac{\mu Q_o(q+2)}{\pi R_{sf}^3} - \tau^*\right), \tag{2.4}$$

where η is a growth rate constant. As the velocity increases (increasing the shear stress), the microscale material in the fluid is less likely to adhere. Thus, for increasing q (progressively tending toward turbulent behavior), there will be less growth (less reduction in R_{sf}). Therefore, we have no growth (or even negative growth) if

$$|\tau_{nw}| = \mu\frac{Q_o(q+2)}{\pi R_{sf}^3} \geqslant \tau^*. \tag{2.5}$$

The steady state value of R_{sf} can be determined by setting $\dot{R}_{sf}=0$, leaving

$$R_{sf}(t=\infty) = \left(\frac{\mu Q_o(q+2)}{\tau^*\pi}\right)^{\frac{1}{3}}, \tag{2.6}$$

[2] Conversely, in locations where one may want growth, for example in a calcium-depleted (bone) region, one could attempt to stimulate growth electrically.
[3] The overall flow rate is assumed constant, $Q_0 = Q$.

which illustrates that, for fixed q, (I) increasing the detachment stress threshold (τ^*) leads to more growth (reduction of R_{sf}), (II) increasing the flow rate (Q_o) leads to less growth and (III) increasing viscosity (μ) leads to less growth. More generally, as the radius of the channel changes, due to wall growth, the flow profile, characterized by q, will change. This is discussed next.

3. Velocity profile changes

The effect of a changing profile is described by representing q by a linear function of the centerline Reynolds' number ($\mathscr{R}_{ec}$)

$$q = q(R_{sf}) = c_1 \mathscr{R}_{ec} + c_2, \tag{3.1}$$

where $\mathscr{R}_{ec} = \frac{\rho v_{max} 2R_{sf}}{\mu}$ and c_1 and c_2 are constants. Models of this type, linking the profile exponent (q) to the centerline Reynolds' number ($\mathscr{R}_{ec}$), are quite well-established, for example, see Hinze [7]. Usually, $0 \leqslant c_1 \ll 1$ and $c_2 \approx 2$, and in the limit we have, for $c_1 = 0$ and $c_2 = 2$, laminar flow. For the general case, combining Eq. (2.2) with Eq. (3.1) and the definition of the centerline Reynolds' number, we obtain a quadratic relationship for q,

$$q^2 - (\lambda + c_2)q - 2\lambda = 0, \tag{3.2}$$

where $\lambda = \frac{2c_1 Q_0 \rho}{\pi k_{sf} \mu}$. This quadratic relationship can be solved in closed form for q to yield

$$q(R_{sf}) = \frac{1}{2}\left((\lambda + c_2) \pm \sqrt{(\lambda + c_2)^2 + 8\lambda}\right). \tag{3.3}$$

Note that for laminar flow ($c_1 = 0$ and $c_2 = 2$) there are two roots to Eq. (3.3), $q = 2$ and $q = 0$. Clearly, the larger root is the correct one.

4. Effects of charging/electrical effects

As before, the shear stress near the wall ($r = R_{sf}$) is given by $\tau_{nw} = \mu \frac{\partial v}{\partial r}|_{r=R_{sf}}$, however, let us now consider a contribution to the growth from the electrical field

$$\dot{R}_{sf} = \eta_1(|\tau_{nw}| - \tau^*) + \text{electrical effects} \stackrel{\text{def}}{=} \mathscr{F}(R_{sf}). \tag{4.1}$$

4.1. Gauss' law for the electric field

Gauss' law provides a useful (conservation) relation between the charge contained within a volume V and the flux of the electric field on a surface A enclosing a volume (cylindrical in the case under consideration)

$$\int_A \boldsymbol{D} \cdot \boldsymbol{n}\, da = \int_V \mathscr{P}\, dv, \tag{4.2}$$

where $\boldsymbol{D}$ is the electric flux density and $\mathscr{P}$ is the charge distribution per unit volume. For a medium obeying a linear constitutive relation, we have $\boldsymbol{D} = \epsilon \cdot \boldsymbol{E}$, where $\boldsymbol{E}$ is the electric field and ϵ is the electric permittivity. We assume that the material is isotropic, $\boldsymbol{D} = \epsilon \boldsymbol{E}$, where $\epsilon = \epsilon_r \epsilon_o$, $\epsilon_o = 8.8542 \times 10^{-12}$ C^2/Nm^2 and ϵ_r is the relative electric permittivity.

4.2. Application to channel flow

For a given value of r (Fig. 2), we employ the integral form of Gauss' law to obtain a z- and θ-independent solution for the electric flux, $\boldsymbol{D} = D\boldsymbol{e}_r$ ($\boldsymbol{e}_r$ is the radial unit vector)

$$\int_A \boldsymbol{D} \cdot \boldsymbol{n}\, da = D 2\pi r L = \int_V \mathscr{P}\, dv = 2\pi L \int_R \mathscr{P}(r)\, r dr \Rightarrow D = \frac{1}{r}\int_R \mathscr{P}(r)\, r dr. \tag{4.3}$$

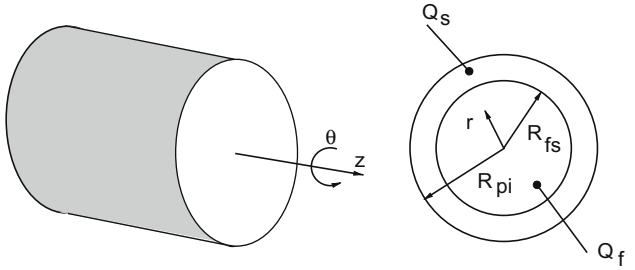

Fig. 2. The charges in the pipe.

For the idealization of a piecewise constant distribution of charge, we have the following (Fig. 2):

- For $0 \leqslant r \leqslant R_{sf}$,

$$D = \frac{1}{r}\int_0^r \mathscr{P}(r)\, r dr = \frac{\mathscr{P}_f r}{2}, \tag{4.4}$$

  where $\mathscr{P}_f$ is the charge of the fluid.
- For $R_{sf} \leqslant r \leqslant R_{pi}$,

$$D = \frac{1}{r}\int_0^r \mathscr{P}(r)\, r dr = \frac{1}{r}\left(\int_0^{R_{sf}} \mathscr{P}(r)\, r dr + \int_{R_{sf}}^r \mathscr{P}(r)\, r dr\right) = \frac{1}{2r}\left(\mathscr{P}_s(r^2 - R_{sf}^2) + \mathscr{P}_f R_{sf}^2\right), \tag{4.5}$$

  where $\mathscr{P}_s$ is the charge of the solid.

Note that since $\boldsymbol{D} = D\boldsymbol{e}_r$, we have, assuming a linear, isotropic material, $\boldsymbol{E} = E\boldsymbol{e}_r$, where $E = D/\epsilon$. Also, note that this solution trivially satisfies the necessary continuity conditions, namely, continuous normal components of $\boldsymbol{D}$ and continuous tangential components of $\boldsymbol{E}$.

4.3. Electrical growth

The electrical force per unit volume produced at the solid-side of the fluid–solid interface is given by $-\mathscr{P}_{s|_{R_{sf}}} E_s \boldsymbol{e}_r$, which collapses to

$$-\mathscr{P}_s E_s = -\mathscr{P}_s \frac{D_s}{2\epsilon_s} = -\mathscr{P}_s \mathscr{P}_f \frac{R_{sf}}{2\epsilon_s}, \tag{4.6}$$

where ϵ_s is the electric permittivity of the solid. If we consider electrical effects alone, we have exponential growth:

$$\dot{R}_{sf} = \eta_2 \mathscr{P}_s \mathscr{P}_f \frac{R_{sf}}{2\epsilon_s} \Rightarrow R_{sf}(t) = R_{sf}(t=0) e^{\eta_2 \frac{\mathscr{P}_f \mathscr{P}_s t}{2\epsilon_s}}, \tag{4.7}$$

where the minus sign has been absorbed into η_2. Clearly, for growth to occur, $\mathscr{P}_f$ and $\mathscr{P}_s$ must be of opposite sign. For the combined effects, one has

$$\dot{R}_{sf} = \mathscr{F}(R_{sf}) = \underbrace{\eta_1(|\tau_{nw}| - \tau^*)}_{\text{mechanical effects}} + \underbrace{\eta_2 \mathscr{P}_s \mathscr{P}_f \frac{R_{sf}}{2\epsilon_s}}_{\text{electrical effects}}. \tag{4.8}$$

4.4. Coupled growth

In order to determine which effect dominates, we form a non-dimensional expression

$$\Theta \stackrel{\text{def}}{=} \left| \frac{\eta_1(|\tau_{nw}| - \tau^*)}{\eta_2 \mathscr{P}_s \mathscr{P}_f \frac{R_{sf}}{2\epsilon_s}} \right|. \tag{4.9}$$

If $\Theta < 1$ then electrical effects dominate the growth, while if $\Theta > 1$ then mechanical effects dominate the growth. The relation in Eq. 4.9 is valid for laminar or turbulent flow. Explicitly, for turbulent flow, we have

$$\Theta \stackrel{\text{def}}{=} \left| \frac{\eta_1\left(\mu \frac{Q_o(q+2)}{\pi R_{sf}^3} - \tau^*\right)}{\eta_2 \mathscr{P}_s \mathscr{P}_f \frac{R_{sf}}{2\epsilon_s}} \right|, \tag{4.10}$$

where $q = q(R_{sf}, Q_0, \mu, \rho, c_1, c_2)$ is given by Eq. (3.3). If we write Eq. (3.3) in the following form

$$q(R_{sf}) = \frac{1}{2}\left((\lambda + c_2) \pm \sqrt{(\lambda + c_2)^2 + 8\lambda}\right) = \frac{1}{2}\left((KR_{sf}^{-1} + c_2) \pm \sqrt{(KR_{sf}^{-1} + c_2)^2 + 8KR_{sf}^{-1}}\right), \tag{4.11}$$

where $K = \frac{2c_1 Q_o \rho}{\pi \mu}$, we observe that

$$q(R_{sf}) = \frac{1}{2}\left((KR_{sf}^{-1} + c_2) \pm \sqrt{(KR_{sf}^{-1} + c_2)^2 + 8KR_{sf}^{-1}}\right) \approx \Lambda_1 R_{sf}^{-p} + \Lambda_2, \tag{4.12}$$

where $0 \leqslant p \leqslant 1$, and Λ_1 and Λ_2 are constants that, in the general case, depend on c_1, c_2, Q_o, ρ and μ. Note that for laminar flow ($c_1 = 0$ and $c_2 = 2$), $\Lambda_1 = 0$ and $\Lambda_2 = 2$. Utilizing Eq. (4.12), we make the following observations:

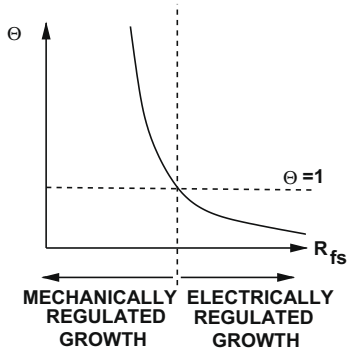

Fig. 3. Qualitative dependence of the growth ratio on R_{sf}.

- Eq. (4.10) implies

$$\Theta \propto \left| A R_{sf}^{-(4+p)} + B R_{sf}^{-4} - C\tau^* R_{sf}^{-1} \right|, \tag{4.13}$$

where $A = \frac{2\eta_1 \mu Q_o \epsilon_s \Lambda_1}{\pi \eta_2 \mathscr{P}_s \mathscr{P}_f}$, $B = \frac{2\eta_1 \mu Q_o \epsilon_s (\Lambda_2+2)}{\pi \eta_2 \mathscr{P}_s \mathscr{P}_f}$ and $C = \frac{2\eta_1 \epsilon_s}{\eta_2 \mathscr{P}_s \mathscr{P}_f}$.

- If we assume the special case of laminar flow

$$\Theta \propto \left| B R_{sf}^{-4} - C\tau^* R_{sf}^{-1} \right|, \tag{4.14}$$

where $B = \frac{8\eta_1 \mu Q_o \epsilon_s}{\pi \eta_2 \mathscr{P}_s \mathscr{P}_f}$ and C remains unchanged.

- If we assume, the special case of zero detachment stress, $\tau^* \approx 0$, along with laminar flow assumption, a very clear trend appears

$$\Theta \stackrel{\text{def}}{=} \left| \frac{\eta_1 8 \mu Q_o \epsilon_s}{\eta_2 \pi \mathscr{P}_f \mathscr{P}_s R_{sf}^4} \right| \propto \frac{1}{R_{sf}^4}, \tag{4.15}$$

which asserts that at smaller radii, the mechanical effects will have a tendency to dominate the growth, while for larger radii, the electrical effects will dominate (Fig. 3).

More precise statements about Θ can only be made by numerically inserting specific parameters into Eq. (4.10).

Remark. We note that the steady state value of R_{sf} can be determined by setting $\dot{R}_{sf} = 0$. This results in the following nonlinear equation for R_{sf}

$$\eta_2 \mathscr{P}_s \mathscr{P}_f \frac{R_{sf}^4}{2\epsilon_s} - \eta_1 \tau^* R_{sf}^3 + \eta_1 \frac{\mu Q_o (q(R_{sf}) + 2)}{\pi} = 0, \tag{4.16}$$

which can be solved via Newton's method for the specific set of parameters chosen.

5. Closing remarks

The developed model illustrates two main effects, namely, for larger scale build up (smaller flow radius), the wall growth is limited by the increase in wall shear stress, due to the more turbulent flow, and for smaller scale build-up (larger flow radius), the effects associated with the electrical field will dominate wall growth.[4] Such an analysis and model provide a useful guide to designing and interpreting long-term experiments, which can take years. Additionally, the model can provide qualitative a-priori guidelines for computationally-intensive large-scale simulations. Generally, in industrial applications involving galvanic protection, it is desirable to keep the degree of electrical intervention to a minimum in order to avoid severe electrical shock and accidental combustion as well as to save power. As mentioned in the beginning of this work, such ideas can, in theory, be applied to biological systems to mitigate, for example, plaque build-up in critical locations within the cardiovascular system. The phenomena of plaque build-up is thought to be due to a relatively high concentration of microscale suspensions (low-density lipoprotein (LDL) particles) in blood.[5] Atherosclerotic plaque formation involves: (I) adhesion of monocytes (essentially larger suspensions) to the endothelial surface, which is controlled by the adhesion molecules stimulated by the excess LDL, as well

[4] Once the growth slows, the cross-section narrows sufficiently to raise the fluid-induced shear stress to a level which exceeds the threshold value of τ^*. As the cross-section narrows, the flow becomes relatively more turbulent, i.e. the Reynolds' number increases as does the exponent q, leading to a more blunted profile.

[5] Plaques with high risk of rupture are termed *vulnerable*.

as the oxygen content and the intensity of the blood flow, (II) penetration of the monocytes into the intima and subsequent tissue inflammation and (III) rupture of the plaque, accompanied by some level of thrombus formation and possible subsequent occlusive thrombosis. For surveys of plaque-related work, see Chyu and Shah [1], Davies et al. [2], Fuster [3], Libby [8–11], Loree et al. [12], Richardson et al. [14], Shah [16] and van der Wal and Becker [17]. The mechanisms involved in the early part of plaque formation (stage (I)), have not been extensively studied, although some qualitative studies have been carried out recently in Zohdi [23] and Zohdi et al. [22], focusing on particle adhesion to artery walls. It is worthy to note that the mechanism for biological attachment is quite involved, and the simple notion used in this paper of a deattachment stress threshold may be inadequate. Therefore, models building upon results such as those found in the extensive works of Hermanowicz and co-workers [4–6,15] may prove quite useful in this regard. This is a subject of current research by the author.

Acknowledgement

The author wishes to thank Prof. Magne Waskaas and Prof. Slawomir Hermanowicz for stimulating discussions on the possible application and extension of the results developed in this work to large-scale water-piping systems, particularly in Norway.

References

[1] K.Y. Chyu, P.K. Shah, The role of inflammation in plaque disruption and thrombosis, Rev. Cardiovasc. Med. 2 (2001) 82–91.
[2] M.J. Davies, P.D. Richardson, N. Woolf, D.R. Katz, J. Mann, Risk of thrombosis in human atherosclerotic plaques: role of extracellular lipid, macrophage, and smooth muscle cell content, Br. Heart J. 69 (1993) 377–381.
[3] V. Fuster, Assessing and Modifying the Vulnerable Atherosclerotic Plaque, Futura Publishing Company, 2002.
[4] S.W. Hermanowicz, A simple 2D biofilm model yields a variety of morphological features, Math. Biosci. 169 (1) (2001) 1–14.
[5] S.W. Hermanowicz, Membrane filtration of biological solids: a unified framework and its applications to membrane bioreactors, in: Proceedings of the Water Environment Membrane Technology 2004 Conference, June 9, 2004, Seoul, South Korea, 2004.
[6] S.W. Hermanowicz, Two-dimensional simulations of biofilm development: effects of external environmental conditions, Water Sci. Technol. 39 (7) (1999) 107–114.
[7] J.O. Hinze, Turbulence, McGraw-Hill, New York, 1975.
[8] P. Libby, Current concepts of the pathogenesis of the acute coronary syndromes, Circulation 104 (2001) 365–372.
[9] P. Libby, The vascular biology of atherosclerosis, in: E. Braunwald, D.P. Zipes, P. Libby (Eds.), Heart Disease. A Textbook of Cardiovascular Medicine, sixth ed., W.B. Saunders Company, Philadelphia, 2001, pp. 995–1009 (Chapter 30).
[10] P. Libby, P.M. Ridker, A. Maseri, Inflammation and atherosclerosis, Circulation 105 (2002) 1135–1143.
[11] P. Libby, M. Aikawa, Stabilization of atherosclerotic plaques: new mechanisms and clinical targets, Nat. Med. 8 (2002) 1257–1262.
[12] H.M. Loree, R.D. Kamm, R.G. Stringfellow, R.T. Lee, Effects of fibrous cap thickness on peak circumferential stress in model atherosclerotic vessels, Circ. Res. 71 (1992) 850–858.
[13] D. Plausinaitis, M. Waskaas, R. Raudonis, V. Daujotis, Piezoelectric resonator and high-frequency admittance study of viscosity and density changes in a thin water layer adjacent to the electrode surface, Electrochim. Acta 51 (27) (2006) 6152–6158.
[14] P.D. Richardson, M.J. Davies, G.V.R. Born, Influence of plaque configuration and stress distribution on fissuring of coronary atherosclerotic plaques, Lancet 2 (8669) (1989) 941–944.
[15] L.K. Sawyer, S.W. Hermanowicz, Detachment of aeromonas hydrophila and pseudomonas aeruginosa due to variations in nutrient supply, Water Sci. Technol. 41 (4–5) (2000) 139–145.
[16] P.K. Shah, Plaque disruption and coronary thrombosis: new insight into pathogenesis and prevention, Clin. Cardiol. 20 (Suppl. II) (1997) II-38–II-44.
[17] A.C. van der Wal, A.E. Becker, Atherosclerotic plaque rupture – pathologic basis of plaque stability and instability, Cardiovasc. Res. 41 (1999) 334–344.
[18] M. Waskaas, Method for Reduction of Flow Resistance in Pipes and Ducts. United States Patent No. US 6,334,957 B1, 2002.
[19] M. Waskaas, Piezometric pressure measurements for water flow in a pipe with electrified inner surface, Russ. J. Electrochem. 42 (12) (2006) 1340–1344 (5).
[20] M. Waskaas, V. Daujotis, K.E. Wolden, R. Raudonis, D. Plausinaitis, Reduction in pressure drop for pipe flow due to applied electric potentials to the pipe, Elektrokhimiya 44 (5) (2008) 649–656.
[21] M. Waskaas, H. Matveyev, K.H. Esbensen, Novel discovery: flow improvement by a particular applied electrical DC-potential. An experimental study, Magnetohydrodynamics 39 (2003) 501–505.
[22] T.I. Zohdi, G.A. Holzapfel, S.A. Berger, A phenomenological model for atherosclerotic plaque growth and rupture, J. Theor. Biol. 227 (3) (2004) 437–443.
[23] T.I. Zohdi, A simple model for shear stress mediated lumen reduction in blood vessels, Biomech. Model. Mechanobiol. 4 (1) (2005) 57–61.